Behaviour of Manganese in Oxide of Fe-Mn-O System†

Nobuya IWAMOTO*, Hiroshi KANAYAMA and Kazumi OGINO*****

Abstract

The behaviour of manganese oxide added in wüstite was investigated with the means of electrical conductivity, X-ray profile analysis, and lattice parameter, and Mössbauer resonance measurements. From the electrical conductivity variation as a function of manganese oxide content at constant temperature and oxygen partial pressure, the different conduction behaviours of three regions were observed.

I. Introduction

The role of slag in the ferrous and nonferrous metallurgy and welding is the most important matter because it plays refining behaviour of impure elements such as sulfur, phosphorus and so on from the molten metals. Although the investigations on the physical properties of the slag in the system MO(or M_2O)-SiO_2 have been done by Bockris and co-workers[1)~4)], the study concerning structure is still inadequate.

Furthermore, the study of transition metal oxides is necessary because they are always included in the slag during the refining processes.

The Fe-O System

Phase diagram on the system Fe-O was accomplished by Darken and Gurry[5)], and the existence of the wider region of wüstite having defect structure has drawn much attention.

Since Koch and C. Wagner[6)] published a paper concerning defect structure of various transition metal oxides, the relationship between semiconducting property and defect structure has been pursued by many investigators[7)~11)]. As for wüstite, the measurements of lattice parameter of the quenched specimen were performed by Jette and Foote[12)], Benard[13)]; and Wills and Rooksby[14)], and Levin and J. B. Wagner [15)], and the decrement of the lattice parameter with the increment of O/Fe ratio were reported. High temperature X-ray measurements were reported by us[16)] and Hayakawa, Cohen and Reed[17)].

Later, the relationship between the value of X in $Fe_{1-x}O$ and P_{O_2} was confirmed by Smyth[18)] and he found that the vacancy concentration is proportional to the 1/6 power of the oxygen pressure using the results obtained by Darken and Gurry[5)]. Himmel, Mehl and Birchenall[19)] and Vallet and Raccah[20)] have reported the similar conclusions. However, from the studies with thermogravimetric means by Swaroop and J. B. Wagner[21)] and with solid electrolyte by Sockel and Schmarzried[22)], it was found that the deviation from the tendency of 1/6 power law in the higher region of oxygen partial pressure occurs.

Likewise, the study of the defect structure was carried on with an electrical conductivity and a thermoelectric measurements. Tannhauser[23)] proposed the electron transfer model between octahedral and tetrahedral sites in the wüstite crystal. Anbrey and Marion[24)] have derived the equation for the electrical conductivity $\sigma=k\{V_{Fe}^{m'}\}$ at the temperature region of 632~916°C, where k and V_{Fe} are constant and the number of iron vacancy, respectively and electron holes m′ produced at the vacancy formation that introduce electrical conduction. Geiger, Levin and J. B. Wagner[25)] have reported that it occurs the transition from 1/6 power low at 1060°C to 1/3.6 power low at 850°C. In the same way, Bransky and Tannhauser[26)] have found the transition of p-to-n type at higher oxygen contents.

On the other hand, Roth[27)] has employed neutron diffraction study for quenched wüstite specimen and he concluded that the movement of cation to the positions of interstitial or tetragonal sites occurs at higher oxygen contents.

Recently, from the studies by thermodynamical, structural and electrical conductivity measurements, the interesting reports which indicated the variation of the defect ordering in the single wüstite phase have appeared.

Vallet and Raccah[20)] have said that there exist in three regions with different structure of wüstite, and that they are based on the vacanct ordering. Fender

† Received on Nov. 25, 1972

* Professor
** Kobe Steel Co. Ltd., Central Research Institute (Formerly Graduate Student at Osaka University)
*** Professor, Dept. of Metallurgy, Faculty of Engineering, Osaka University

and Riley[28], who used electrochemical means, have found that there exist three regions depending on order-disorder transformation in despite of some differences from the result of Vallet and Raccah[20].

The Mn-O System

As for the system Mn-O, MnO, Mn_2O_3 and MnO_2 are known to exist as stable phases. Comprehensive study of MnO phase was performed by Davis and Richardson[29], who found the O/Mn ratio of MnO depends on oxygen partial pressure and the ratio change from unity to 1.045. Dusquenoy and Marion[30] found that MnO may be p-type or n-type depending upon the oxygen partial pressure over the temperature range 900-1200°C and they derived the defect model. Hed and Tannhauser[31] determined the MnO-Mn_3O_4 phase boundary and showed the relationship between isotherms of the electrical conductivity and $\log[P_{CO_2}/P_{CO}]$ at constant temperature and found that the conductivity of MnO behaves differently in three regions. Eror and J. B. Wagner[32] studied the nonstoichiometric disordering in single crystalline MnO and concluded that the behaviour of MnO is different in only two regions controversial with regard to the existence of three regions described above and both of them fit to $\pm 1/6$ power law.

The Fe-Mn-O System

It is found that a complete solid solution between MnO and FeO can be formed. However, according to our experiment[33] as for non-metallic inclusions manganese killed steel, no clear solution from the formation of their simple solid solution has been given. For this reason, there is a difficulty that FeO as well as MnO is apt to solve in the extraction process. In general, iodine-alcohol solution is used as extracting agent to steel. We used special agent for mild extraction, and various inclusions were determined. It is important to study on the behaviour of the binary oxide in order to know the deoxidation property of manganese in steels.

In this paper, electrical properties of binary oxide having various Fe/Mn ratios were investigated. For comparison with previous studies, thermogravimetric and defect structural studies as for wüstite have been done.

Furthermore, to obtain the information as for defect structure of wüstite and mangano-wüstite, X-ray diffraction profile analysis, high temperature X-ray diffraction and Mössabauer resonance studies were performed.

2. Experimental Procedures

Hematite made from ferrous oxalate and Mn_3O_4 obtained from manganese carbonate as the starting materials were used.

To get mangano-wüstite having various ratio of Fe/Mn, both were throughly mixed in aceton and they were heattreated at 1400°C for 1 hr in Pt crucible. According to Muan and Somiya[34], complete solid solution between them is formed at 1400°C in air. Chemical analysis of these materials was performed by emission spectroscopy. Impure elements, which have great effect on the electrical property, were compared with standard Spex Mix. The experimental conditions and the results are given in **Table 1.**

Table.1. Chemical analysis of starting materials (%).

	Si	Ca	Mn	Fe	Mg	Cu	Al	Cr
Mn_3O_4	0.00002	0.0192	—	nil	+	—	—	—
Fe_2O_3	0.083	0.0256	0.256	—	+	++	+	+—

Exp, Conds.
Apparatus, Evert type spectrometer (Shimazu Seisaku Co. Ltd.)
High resolution spectrometer type III (〃)
Emission stand type 9010 (Spex Co. Ltd.)
Plate, Kodak sA—1 Grating, 1200 lines/mm (2.4 Å/mm)
Secondary voltage, 200 V Secondary current, d—c 5 A
Slit width, 20 μ Analysis interval, 4 mm Sample side, (+)
Electrode, 3 mmϕ ×3 mm Exposure, 30 sec Atm., in air

The sintered specimens were recrushed in aceton, and the particle size was controled. The specimen having 12 mm cube was formed under the pressure of 6 ton/cm^2 and it was re-heattreated at 1400°C for 1 hr. For the measurement of porosity, apparent density by JIS M8716 and true density by modified JIS M8716 were determined. Porosity can be calculated with following equation,

$$P=(S_t-S_A)/S_t\times 100$$

where p is porosity (%), S_t is true density and S is apparent density. The results obtained are given in **Table 2.**

Table 2. Specific gravity and porosity of the specimens

Fe/Mn	S_t	S_A	P (%)
*10/0	5.48	3.66	33.3
* 9/1	5.60	4.20	25.1
7/3	4.76	3.94	17.2
5/5	4.89	3.86	21.1
4/6	4.77	3.56	25.3
* 2/8	5.34	3.49	34.7
* 0/10	5.24	3.32	36.8

* denotes specimen after experiment.

To exclude contact resistance of the specimen, Pt paste was used, which is made from powdered Pt of 100~250 mesh and non-ionic surface agent and ethyl alcohol solution.

Both surfaces of specimen was washed and slowly heated to 1400°C and holded for 1 hr. And then, Pt paste was rewashed and Pt plate (20 mmϕ, 0.2 mm thickness) was laid on the specimen and the similar heat-treatment was repeated. Two Pt wire (0.5 mmϕ) were spot-welded to Pt plate and led to the measuring circuit. Upper electrode was depressed with spring. D-c method was applied and voltmeter (Yokogawa Hewlet Packard Model 4304A) and standard resistor (0.1 Ω, 10 Ω) were used. Electrical current of about 100 mA was passed to electrode. Experimental apparatus is shown in **Fig. 1.**

Thermogravimetric measurement was done with semi-micro balance (Chōu Keiryōki Co. Ltd.).
Various mixed gases, H_2, CO_2 and CO, were supplied by Seitetsu Chemical. They were ultrapure grade. Mixed gases having various ratio of CO_2/CO, 9/1, 4/1, and 1/1 and 1/4, were offered by the maker too. Chemical analyses of gases are given in **Table 3.** Gases having miscellaneous ratios were produced by gas mixer[35].

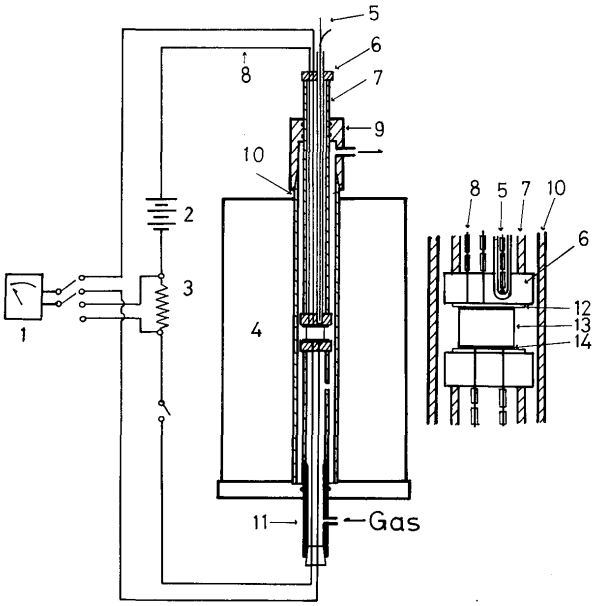

Fig. 1. Apparatus for Conductivity Measurement.
1. Voltmeter 2. Battery 3. Standard Resistance 4. Pt.-Furnace 5. Thermocouple 6. Al_2O_3-Plate 7. 10 Al_2O_3-Tube 8. Pt-Wire 9. Brass Jaket 11. Brass Tube 12. Pt-Plate 13. Specimen 14. Pt-Paste

Table 3. Chemical analysis of gases used. (ppm)

	H_2O	O_2	CH_4	H_2
CO_2	—	2	20	—
H_2	tr.	2—3	—	99.9 %

To confirm profile analysis of X-ray diffraction, wüstite and mangano-wüstite specimens were quenched into ice-cooled meacury after kept at 1350°C in the solid state and at 1500°C in the liquid state for 1 to 5 hrs. CoKα radiation filtered with iron was used. To take off the X-ray instrumental errors, silicon powder as the standard specimen was used. Each line profiles of (111), (200) and (200) were obtained with the fixed count method. To obtain accurate profiles of higher order diffraction of mangano-wüstite, the most intense X-ray diffraction was used. Fourier analysis by Stokes[36] was carried out with computor and the integrated intensity was calibrated with the values already given[9), 36~38].

High temperature X-ray diffraction was performed with photographic method by Rigaku high temperature camera (type 1211/M2).

The electrical conduction measurement of wüstite melt under the various oxygen partial pressures were carried out at 1500°C with d-c four terminal method. Pt-20 %Rh crucible was used. Cell constant was obtained with IN potassium chloride aqueous solution. Electrical conductivity κ was calculated from the following equation

$$\kappa=(I/V)\cdot(1/s)$$

,where κ is the electrical conductivity (mho/cm), I is the intensity (A), and V is the voltage (V) and 1/s is the cell constant (cm^{-1}) respectively. Experimental apparatus is shown in **Fig. 2.**

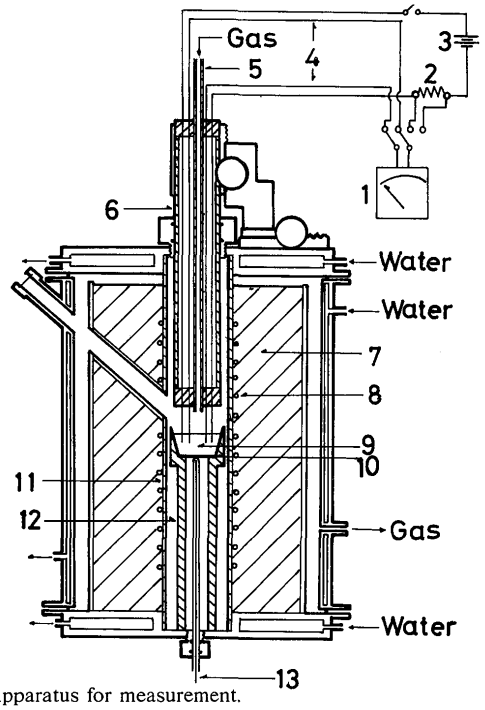

Fig. 2. Apparatus for measurement.
1. Volt meter 2. Standard reesistance 3. Battery 4. Pt-wire 5, 6, 11, 12. Al_2O_3-tube 7. Bubbled Al_2O_3 8. Pt-furnace 9. Melt 10. Pt-crucible 13. Thermocouple

The Mössbauer spectrometer is composed of the electromagnetic velocity and the γ-ray counting systems. The Mössbauer resonance analyzer (Elron #5011) of the linear velocity type connected to a multichannel analyzer. The source of γ-ray is ^{57}Co (5 and 30 m Ci) diffused into stainless steel and palladium and are attached to the velocity transducer to provide Doppler shift. The line width observed with the source against thin iron foil absorbers was 0.35 mm /sec.

A proportional counter filled with a mixed gas of 95 %Xe and 5 %N_2 was used for the detection of 14.4 KeV γ-ray. The velocity scale was calibrated with pure iron as a standard absorber. Specimens used for this experiment are given in **Table 4.**

Table 4. Composition of specimens and the isomer shift values (δ)

Specimen	Temp (°C)	Holding Time (Hr)	Mn (%)	CO_2/CO	δ
W —1	1350	1	0	1/1	1.000
WM—1	1350	1	1	4/1	1.0104
WM—2	1350	1	3	4/1	0.9792
WM—3	1500	1	0.5	4/1	0.9792
WM—5	1500	3	3	4/1	0.9354

Theory[7]

FeO and MnO are oxygen-excess compounds over the most of their range of existence. From the difference of the ionic radii between metallic cation and oxygen, metal vacancies may be introduced through the reaction of oxygen with the oxide

$$1/2O_2 = V_M^X + O_0 \quad (1)$$

Correspondingly, the metal vacancy with one or two effective negative charges and one or both of the holes are formed depending on the temperature

$$V_M^X = V_M' + h^{\cdot} \text{ ,etc.} \quad (2)$$

The defect equilibria describing the formation of single neutral metal vacncies and the subsequent excitation of electron holes in MO may be expressed for small defect concentration

$$[V_M^X] = K_1 P_{O_2}^{1/2} \quad (3)$$
$$[V_M'] p = K_e [V_M^X] \quad (4)$$
$$[V_M''] p = K_f [V_M'] \quad (5)$$

where $p=[h^{\cdot}]$ denotes the concentration of electron holes.

From the electroneutrality conditions, it leads

$$P = [V_M'] + 2[V_M''] \quad (6)$$

Through combinations of Eq. 3—6 the concentration of the separate point defects and p can be evaluated.

$$P^3 = K_1 K_e P_{O_2}^{1/2} (2K_f + p) \quad (7)$$

As for oxygen vacancies, two limiting conditions must be considered. (1) At low values of p ($p \ll 2K_f$), then

$$P = (2K_1 K_e K_f)^{1/3} P_{O_2}^{1/6} \quad (8)$$

while at (2) high values of p ($p \gg 2K_f$), then

$$p = (K_1 K_e)^{1/2} P_{O_2}^{1/4} \quad (9)$$

The total concentration of the metal vacancies correspondingly changes from $P_{O_2}^{1/6}$ through $P_{O_2}^{1/2}$.

CO_2-CO Equlibrium[39]

From the equilibrium reaction,

$$2CO_2(g) = 2CO(g) + O_2(g)$$

the equilibrium constant K is obtained as follows:

$$K = P_{O_2} \cdot P_{CO}^2 / P_{CO_2}^2$$

At constant temperature,

$$P_{O_2} = 1/K \cdot (P_{CO_2}/P_{CO})^2$$

so the following relation is obtained

$$\log P_{O_2} \propto 2 \log P_{CO_2}/P_{CO}$$

3. Experimental Results and Discussions

Thermogravimetric Study of Wüstite

The nonstoichiometry as a function of temperature and oxygen partial pressure has been studied by several investigators[7)~11)]. All the papers have recognized that linear relationship between them exists. **Fig. 3** shows the variation of O/Fe ratio as a function of P_{O_2} at various temperatures. Linear changes of O/Fe ratio were verified in agreement with the previous findings. However, the value of P_{O_2} equilibrating with FeO having the decided defect structure is somewhat different from the value by Darken and Gurry[5]. Using H_2/CO_2 mixed gas, thermal segregation in the

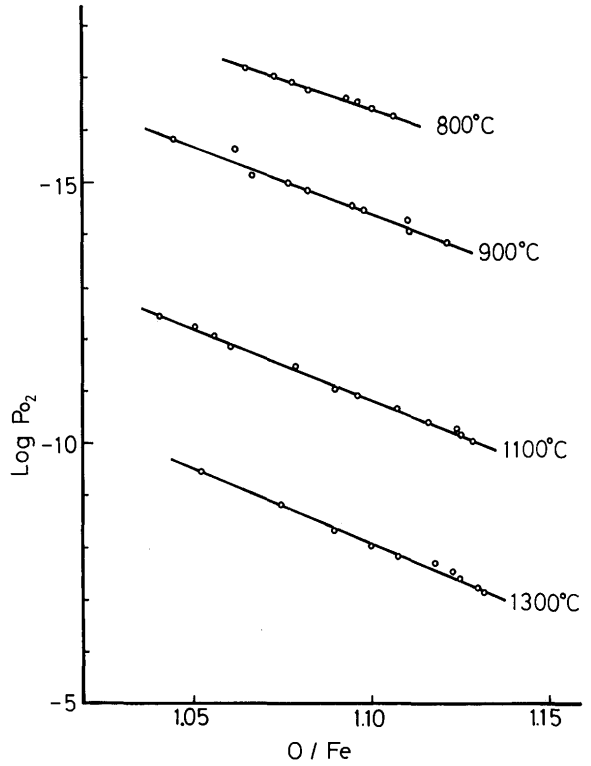

Fig. 3. Variation of O/Fe as a function of P_{O_2} at various temperatures.

gases probably occurs. On the thermogravimetric study, CO_2/CO mixed gas does not use, because it necessitates refractory tube having large caliber and to avoid leak of toxic gases.

Figure 4 shows cation deficiency as a function of the oxygen partial pressure as for FeO. The vacancy concentration is proportional to the 1/6 power of the oxygen partial pressure and hence the reaction establishing the nonstoichiometry is

$$1/2\ O_2 = O_0 + V''_{Fe} + 2\oplus,$$

,where the symbol, V''_{Fe} , denotes a cation vacancy with no associated electron holes, and the symbol, $\oplus$, denotes an electron hole. Sockel and Schmarzried[22] have reported that the slope of 1/6 power begins to deviate and reaches to the slope of 1/8 power where wüstite-magnetite transition occurs. Likewise, Swaloop and J. B. Wagner[21] have supported this finding. In our results, the same behaviour of the slope was found. For this deviation from 1/6 to 1/8 power, the following reason should be considered. It is emphasized that the equilibrium constant relates the activities of the structure elements involved in the defect reaction, but under ideal conditions and when the structure elements can be assumed to be randomly distributed over available sites, the activities are equal to the concentrations of the structure elements. This is a valid assumption in dilute solutions. However, when ordering of defects occurs or when the defects are not randomly distributed due to mutual interactions of the defects, etc., the activities have to be used instead of concentrations. Raccah and Vallet[20], Carel and Vallet[41] and Carel, Wiegel and Vallet[42] have reported that there are three different regions within FeO domain labeled I, II and III. The existence of three different regions may be associated with order-disorder transitions, but the viewpoint of structure as for transition is an open question. As an example, the time for the equilibrating in the thermogravimetric studies is shown in **Fig. 5.** It is anticipitated that the longer time is necessary to carry out the reducing experiment from magnetite to wüstite.

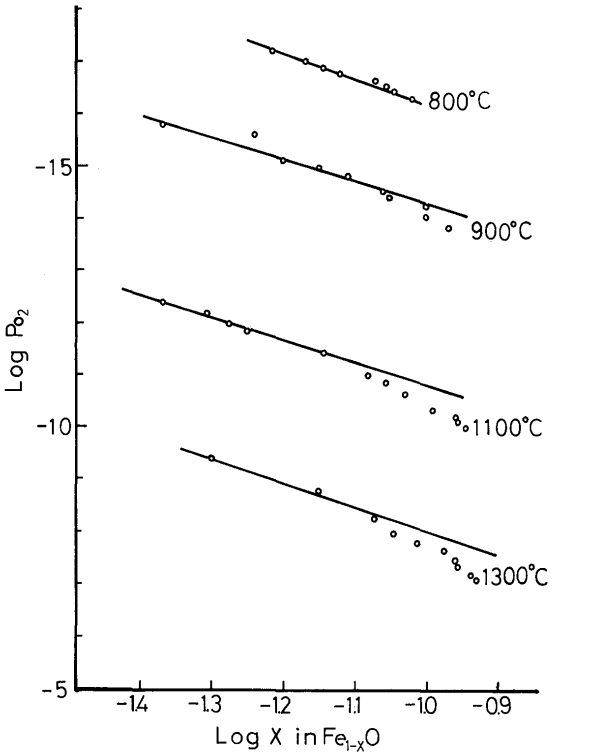

Fig. 4. Cation deficiency, Log X, in $Fe_{1-x}O$ as a function of Log P_{O_2}.

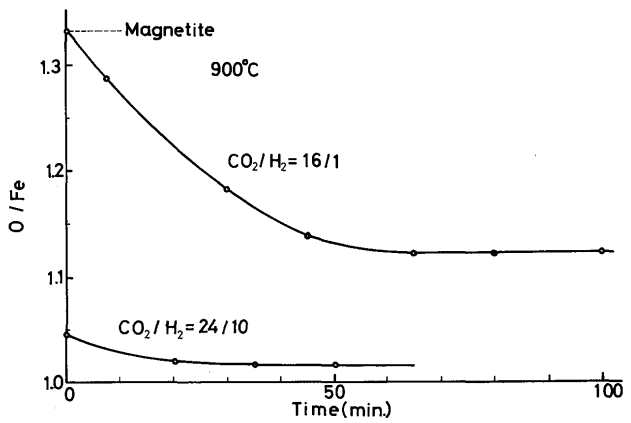

Fig. 5. Variation of O/Fe with time.

Electrical Conductivity

Figure 6 and **7** show electrical conductivity results of mangano-wüstite having various ratio of Fe/Mn as a function of the partial pressure of oxygen (ratio of P_{CO_2}/P_{CO}) at 1300°C. Curve 1 shows the change of $\log\sigma$ between 1.5～1.8. Geiger, Levin and J. B. Wagner[25] have reported the change of $\log\sigma$ between 1.93—2.25 at 1000°C. It is appropriate value because of $\log\sigma$ wüstite becomes greater with the rise of temperature. However, the difference of the specimens used should be considered. They corrected thickness of sample by using initial thickness and lattice constant of wüstite, and the influence of porosity may be important in our case. In the region of low oxygen partial pressure, it is seen that $\log\sigma$ is proportional to 1/6 power of P_{O_2} but it is apparent from curve 1 that plots of $\log\sigma$ tend to exhibit curvature at the higher oxygen concentrations as well as the results obtained by the thermogravimetric study.

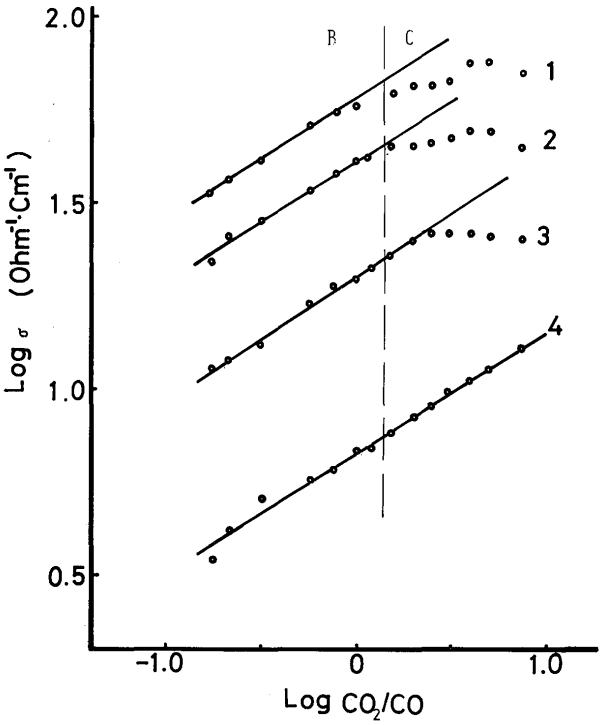

Fig. 6. Electrical conductivity on various composition of mangano-wüstite at 1300°C.
Fe/Mn ratios (1) 10/0, (2) 9/1, (3) 8/2, (4) 6/4.

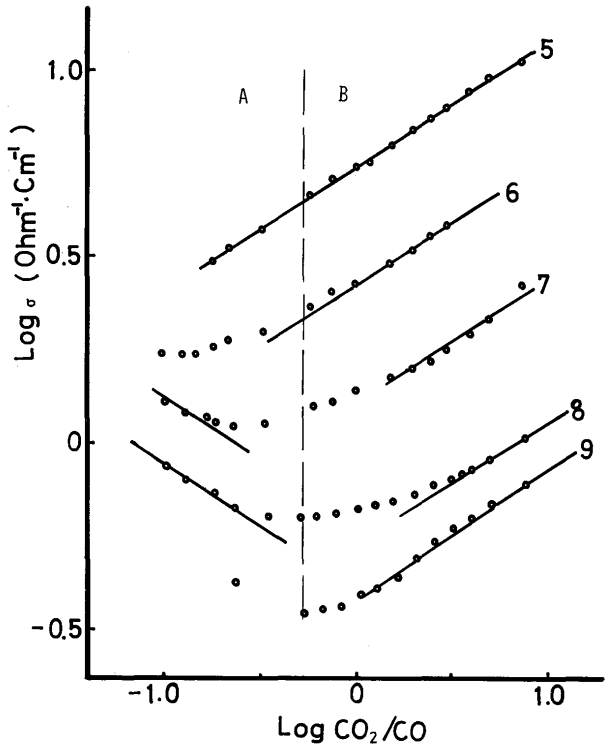

Fig. 7. Electrical conductivity on various composition of mangano-wüstite at 1300°C.
Fe/Mn ratios (5) 5/5, (6) 7/3, (7) 2/8, (8) 1/9, (9) 0/10.

The curve approaches to the maximum value and shows transition. This is the representation of p-to-n transition of wüstite. The interpletation of this transition mechanism are not tenable. However, the defect structural models presented must be examined. Neutron diffraction study by Roth[27] indicated that the defects in wüstite could be considered as "micro-domains" of magnetite in wüstite. From the further studies of superstructure peaks from wüstite, the presence of long-range order have been suggested[43),44)]. With the increase of manganese content in mangano-wüstite, the linear relation of 1/6 power law are notable as shown at the curves 4 and 5. With further increase of manganese content, p-to-n transition appears at the lower oxygen partial pressure. This finding is in agreement with the previous results.

Until now, Dusquenoy and Marion[30], Hed and Tannhauser[31], and Eror and J. B. Wagner[32], and O'Keeffe and Valigi[45], and Bocquett, Kawahara and Lacombe[46] have studied the electrical conductivity of MnO as a function of temperature and oxygen partial pressure. They verified p-to-n transition with the minimum value of $\log\sigma$ at $CO_2/CO=1/1$. The regions which show different behaviours of electrical conductivity have been termed A, B and C (These are described in **Fig. 6** and **7**). At partial pressures lower than that of the minima (region A) the conductance increases with decreasing pressures, and the oxide is n-conductor, while at higher partial pressures the oxide is p-conductor and the conductivity increases with increasing oxygen pressure. On the other hand, the oxygen partial pressure dependence of the conductivity in which n-type conduction occurs gives $CO_2/CO=1/7.5$, and the value is consistent with the value by Hed and Tannhauser[31] as for MnO at 1200°C. The clear interpretation of this dependence is not given as well as the abnomal behaviour at higher oxygen partial pressure region.

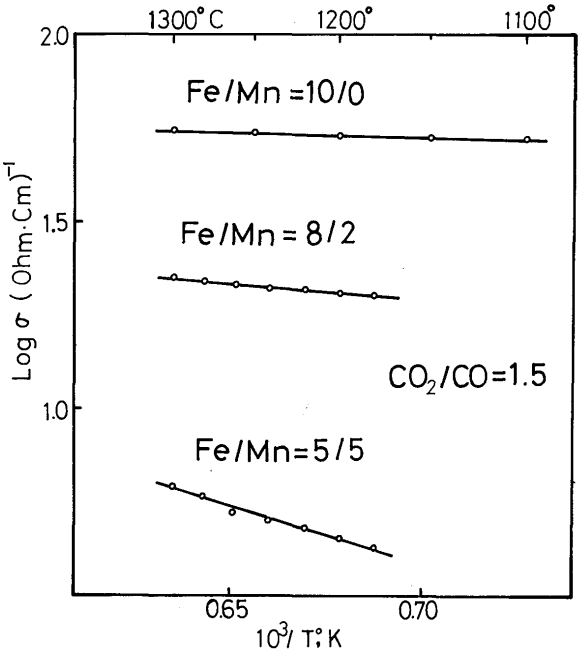

Fig. 8. Variation of electrical conductivity as a function of temperature.

Figure 8 shows electrical conductivity of manganowüstite having various ratio of Fe/Mn as a function of temperature at constant oxygen partial pressure. From this, it is verified that the conduction behaviour are different between the content of Fe/Mn=10/0, 8/2 and 5/5.

Figure 9 shows the electrical conductivity variation as a function of manganese oxide added at constant temperature and oxygen partial pressure. Likewise, the different conduction behaviours of three groups are anticipitated.

To explain the different electrical conduction behaviours, structural experiment has been necessitated.

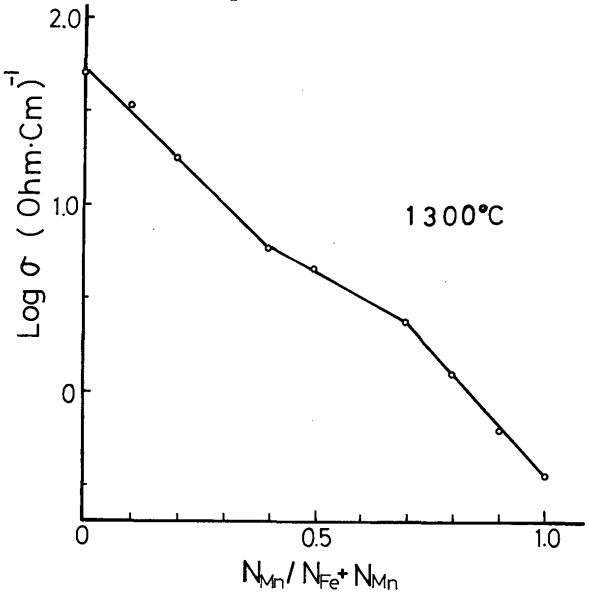

Fig. 9. Variation of conductivity as a function of Mn concentration at CO_2/CO=0.5.

X-ray Profile Analysis

The defect structure of wüstite has been studied by measuring the integral X-ray intensity of powders quenched from solidus and liquidus regions. The co-existing phase in the specimens used is shown in **Table 5.** It is apparent that the longer holding time than 3 Hrs. is necessary to bring these specimens to equilibrium. One would expect the effect of instrumental error on the X-ray diffraction profiles from the comparison of h (x) measured with f (x) treated with Fourier analysis in **Tables 6** and **7.** As an example, line profiles of f (x) of specimens are given in **Fig. 10.** Structure factor calculated as wüstite takes spinellike structure is given in **Table 8.** The distribution of Fe^{3+} between octahedral and tetrahedral sites denoted by parameter y introduced by Roth[27] and Smuts[37] was taken into the calculation. For comparison, structure factor

Table 5. Sample compositions and co-existing phase

Specimen	Temp (°C)	Holding Time (Hr)	Mn (%)	CO_2/CO	Phase
W —5	1350	1	0	4/1	Magnetite
W —9	1500	5	0	4/1	—
WM—1	1350	1	1	4/1	Magnetite
WM—2	1350	1	3	4/1	Magnetite
WM—3	1500	1	0.5	4/1	Magnetite
WM—4	1500	3	3	1/4	Tr. Magnetite
WM—5	1500	3	3	4/1	—

Table 6. Breadth of h(x).

Specimen	(111)	(200)	(220)
W —5	0.27°	0.29°	0.43°
W —9	0.24	0.31	0.32
WM—1	0.24	0.28	0.36
WM—5	0.21	0.23	0.37

Table 7. Breadth of f(x).

Specimen	(111)	(200)	(220)
W —5	0.16°	0.14°	0.25°
W —9	0.16	0.18	0.16
WM—1	0.16	0.17	0.21
WM—5	0.13	0.16	0.20

Table 8. Structure factor ratio.

Specimen	$\lvert F_{200}\rvert^2/\lvert F_{111}\rvert^2$	$\lvert F_{220}\rvert^2/\lvert F_{111}\rvert^2$
$Fe_{1.0}O$	2.93	1.87
$Fe_{0.9}0$	1.87	2.06

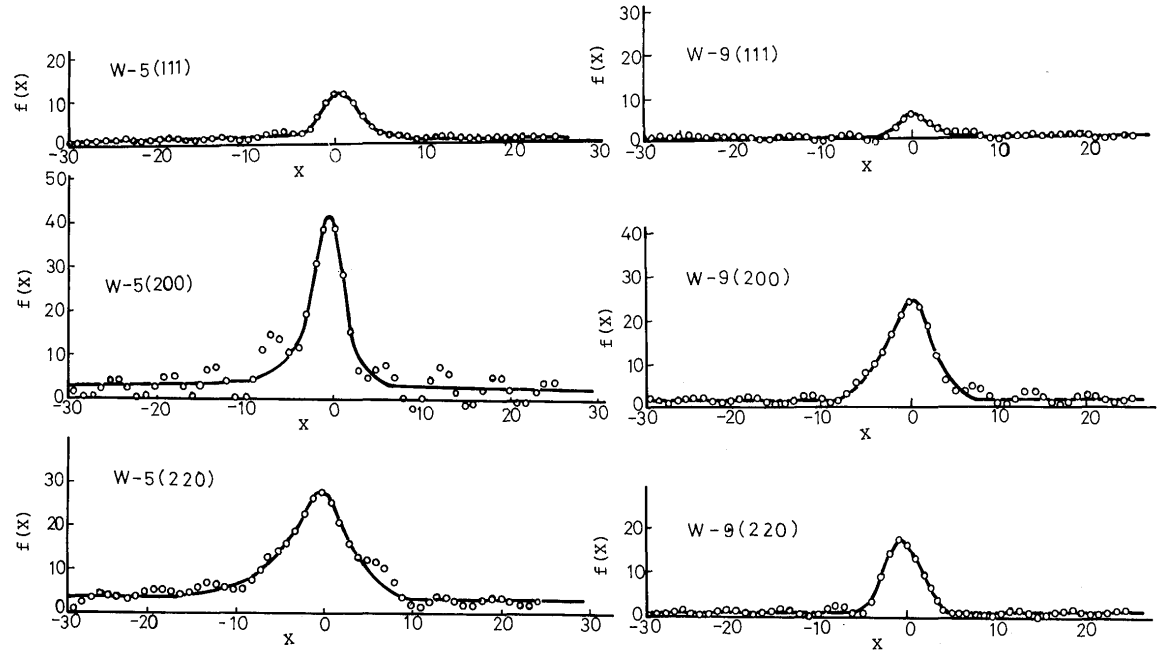

Fig. 10 (a). Profile obtained from fourier analysis.

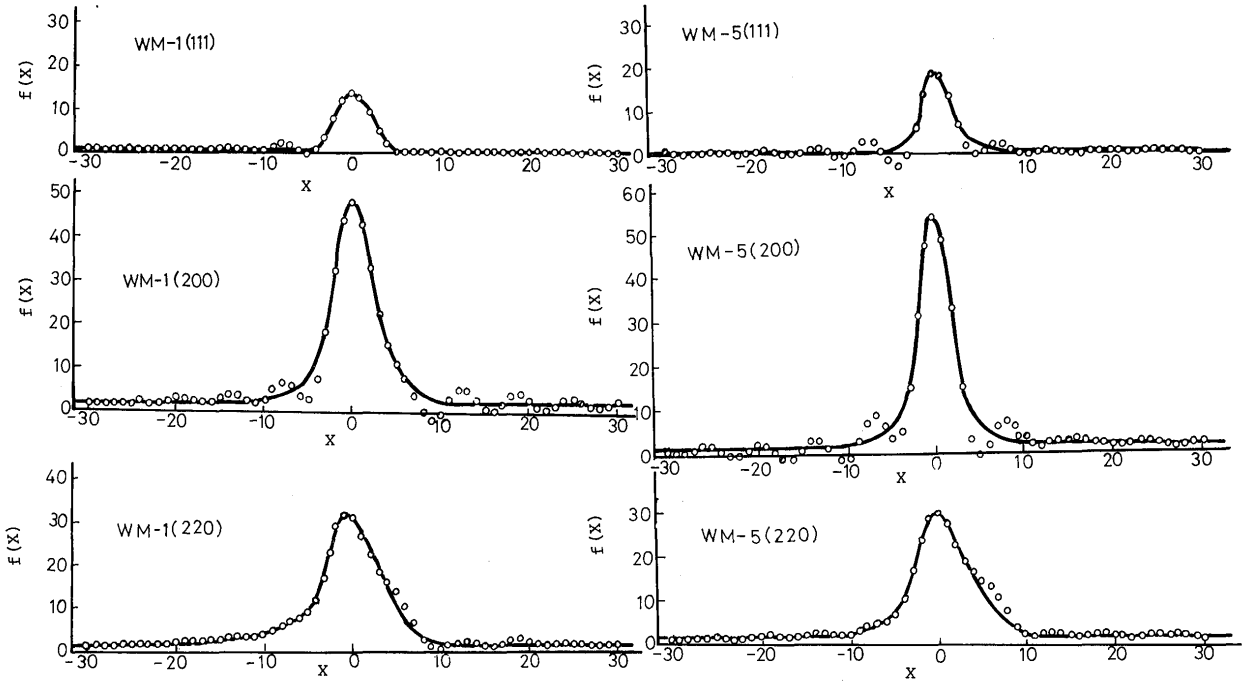

Fig. 10 (b). Profile obtained from fourier analysis.

calculated as taking sodium chloride structure ($Fe_{10}O$) is given too. In **Table 9,** the structure factor of each specimens are represented. The inconsistency is remarkable to decide what model is apposite to wüstite, so it should be considered if any abnomal situation of X-ray reflection occurs on (111) plane. From the mean dimention of the crystallite of each planes calculated from Scherrer's equation[47] in **Table 10,** but it was impossible to interplet the cause of the differences. Although another reflections of the higher planes were desired, they were insufficient on account of their weak reflections. Notable difference was not

Table 9. Structure factor ratio

Specimen	$\lvert F_{200}\rvert^2/\lvert F_{111}\rvert^2$	$\lvert F_{220}\rvert^2/\lvert F_{111}\rvert^2$
W —5	6.77	7.92
W —9	10.03	6.75
WM—1	7.38	8.03
WM—5	7.11	5.56

Table 10. Mean dimension of crystallites (Å).

Specimen	D_{111}	D_{200}	D_{220}
W —5	735	868	562
W —9	735	648	818
WM—1	744	684	644
WM—5	888	764	867

appreciated to specimens quenched from the molten state and the influnce of manganese addition was not noticed too. In order to get X-ray profiles of the higher order reflection of mangano-wüstite, more intense X-ray diffraction were used. Profile analysis results of this experiment will be published in near future.

Lattice Parameter Study

The lattice parameters obtained from the quenched specimens are given in **Table 11.** The important fact of the lattice parameter in mangano-wüstite melt is independent of the manganese content and oxygen partial equilibrated.

Table 11. Lattice parameter of specimens (Å).

Specimen	a_0	Specimen	a_0
W —5	4.278_0	W —9	4.277_4
WM—1	4.285_8	WM—3	4.285_2
WM—2	4.290_7	WM—4	4.285_2
		WM—5	4.285_2

High Temperature X-ray Diffraction Study

Results of high temperature X-ray diffraction are given in **Table 12.** We could not agree that magnetite and wüstite are continuous phases[37] from the facts, their similtaneous appearence at 800°C when CO_2/CO ratio is 4/1, different expansion behaviours and electrical conductivity change. Interplanar spacings of wüstite and magnetite under various experimental conditions are given in **Table 13.**

Table 12. Results of high temperature X-ray diffraction.

CO_2/CO	Temp.(°C)	Phases
9/1	1300	M
	1200	M
	1100	M
	1000	M
4/1	1250	W
	1100	W
	1000	W
	900	W
	800	W+M
	600	M
	500	M
1/1	1000	W
	900	W
	800	W
1/4	1100	γ—Fe

W: wüstite, M: magnetite

Table 13 (a) Interplanar spacings of magnetite (Å).

(hkl)	Standard value	Sp. quenched	High temp. diff.	
		CO_2/CO=9/1 1300°C	CO_2/CO=9/1 1000°C	CO_2CO=9/1 1200°C
220	2.963_8	2.982_7	3.016_0	3.011_6
311	2.530_5	2.533_8	2.570_9	2.591_1
400	2.097_0	2.104_6	2.122_3	2.130_6
422	1.711_9	1.717_3	1.729_6	1.734_8
511	1.613_1	1.618_4	1.634_8	1.636_6
440	1.482_7	1.491_3	1.498_1	1.499_6

Table 13 (b). Interplanar spacings of wüstite (Å).

(hkl)	Sp. quenched	High temp. diff.		
	CO_2/CO=4/1	CO_2/CO=1/1	CO_2/CO=4/1	
	1300°C	1000°C	900°C	1100°C
111	2.486_2	2.525_2	2.518_4	2.518_8
200	2.148_6	2.186_9	2.173_7	2.175_9
220	1.517_2	1.541_2	1.536_3	1.540_8
a_0	4.287_0	4.347_5	4.347_5	4.350_7

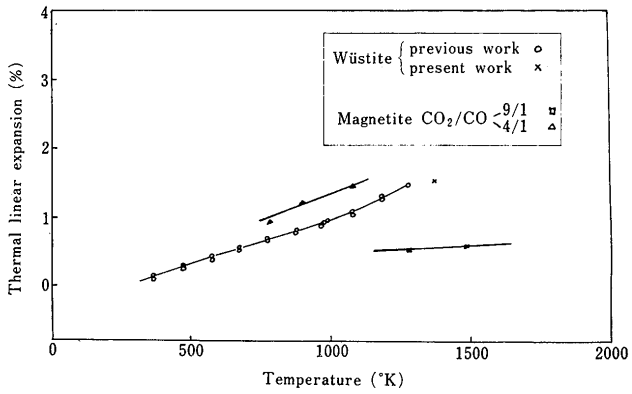

Fig. 11. Thermal linear expansion values of wüstite and magnetite.

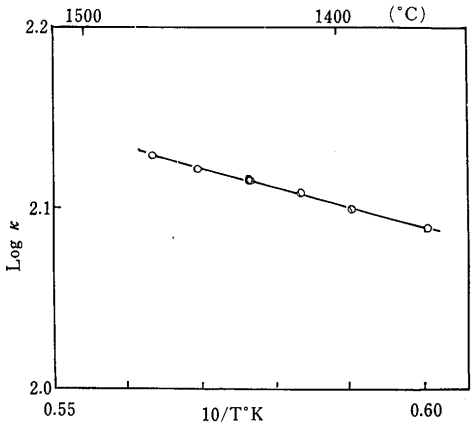

Fig. 12. Variation of electrical conductivity of wüstite melt as a function of temperature.

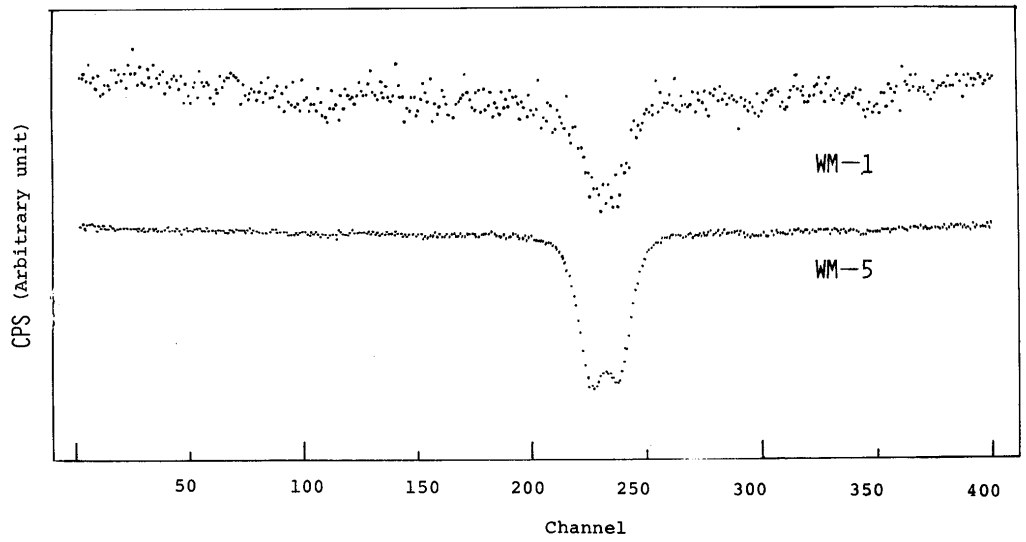

Fig. 13. Mössbauer spectra of mangano-wüstite.

The thermal linear expansion coefficient calculated from high temperature X-ray diffraction analysis was compared with the value obtained from usual expansion experiment[48]. Good agreement as for wüstite was determined, but some irregularities were certified in magnetite. These tendencies are shown in **Fig. 11.**

Electrical Conductivity of Wüstite Melt

The dependency of the electrical conductivity on the oxygen partial pressure of wüstite melt was not determined.

It must be considered that the corrosion of Pt-20 %Rh crucible used occurs, so the choice of sample holder is necessitated. Result obtained is shown in **Fig. 12.** Semi-conduction characteristic and the value of conductivity have shown good agreement with the value previously given[49].

Mössbauer Resonance Study

Mössbauer spectra of mangano-wüstite are shown in **Fig. 13.** In **Table 14,** isomer shift values are given. Profile analysis to separate two quadrupole splits Fe^{2+} and a Fe^{3+} singlet is now proceeding. In near future, the information as for defect structure will be published.

4. Summary

The behaviour of manganese oxide added in wüstite was studied with various physical methods. From the electrical conductivity measurement, it was anticipitated that there are three regions which show different conduction tendency with the manganese oxide content in wüstite. With the results obtained

from X-ray diffraction profile analysis, Mössbauer resonance analysis and so on, the abnormal behavior of manganese will be clarified in future.

Acknowledgments

The authors wish to express their thanks to Sumitomo Metal Central Research Institute for their assistances in the emission spectroscopy and to Kobe Steel Central Research Institute for porosity measurement and to Shimazu Seisakusho in the Mössbauer resonance study and to Seitetsu Chemical for special gases supports.

References

1) J. O'M. Bockris, J. A. Kitchener and A. E. Davis: *Trans. Faraday Soc.,* **48** (1952), 536.
2) J. O'M. Bockris and D. C. Lowe: *Proc. Roy. Soc.,* **A226** (1954), 423.
3) J. O'M. Bockris, J. D. Mackenzie and J. A. Kitchener: *Trans. Faraday Soc.,* **51** (1955), 1734.
4) J. W. Tomlinson, M. S. Heynes and J. O'M. Bockris: ibid, **54** (1958), 1822.
5) L. S. Darken and R. W. Gurry: *J. Am. Chem. Soc.,* **67** (1945), 1398, **68** (1946), 798.
6) E. Koch and C. Wagner: *Z. Phys. Chem.,* **B32** (1936), 439.
7) F. A. Kröger and H. J. Vink: "Solid State Physics" Ed. by F. Seitz and D. Turnball, **3** (1956), Academic Press, New York.
8) F. A. Kröger: "The Chemistry of Imperfect Crystals" North-Holland Publ. Co. Amsterdam, & Wiley, New York 1964.
9) W. van Gool: "Principles of Defect Chemistry of Crystalline Solids" Academic Press, New York, 1966.
10) R. F. Gould ed.: "Non-stoichiometric Compounds" Amer. Chem. Soc., New York, 1963.
11) L. Mandelcorn ed.: "Non-stoichiometric Compounds" Academic Press, New York, 1964.
12) E. R. Jette and F. Foote: *J. Chem. Phys.,* **1** (1933), 29.
13) J. Benard: *Bull. Soc. Chim.,* **16** (1949), D109.
14) B. T. M. Willis and H. P. Rooksby: Acta. Cryst., **6** (1953), 827.
15) R. L. Levin and J. B. Wangner: Trans. AIME, **236** (1966), 516.
16) N. Iwamoto, H. Kanayama and K. Ogino: *Proc. I. C. S. T. I. S.,* (1971), 491.
17) M. Hayakawa, J. B. Cohen and T. B. Reed: *J. Am. Ceram. Soc.,* **55** (1972), 160.
18) D. M. Smyth: *J. Phys. Chem. Solids,* **19** (1961), 167.
19) L. Himmel, R. F. Mehl and C. E. birchenall: *Trans. AIME,* **197** (1953), 822.
20) P. Vallet and P. Raccah: *Mem. Sci. Rev. Met.,* **62** (1965), 1.
21) B. Swaloop and J. B. Wagner: *Trans. AIME,* **239** (1967), 215.
22) H. G. Sockel and H. Schmalzried: *Ber. Bunsengesengesellschaft,* **72** (1968), 747.
23) D. S. Tannhauser: *J. Phys. Chem. Solids,* **23** (1962), 25.
24) J. Anbrey and F. Marion: *Compt. Rend.,* **241** (1955), 1778.
25) G. H. Geiger, R. L. Levin and J. B. Wagner: *J. Phys. Chem. Solids,* **27** (1966), 947.
26) I. Bransky and D. S. Tannhauser: *Trans. AIME,* **239** (1967), 75.
27) W. L. Roth: *Acta. Cryst.,* **13** (1960), 140.
28) B. E. F. Fender and F. D. Riley: *J. Phys. Chem. Solids.,* **30** (1969), 793.
29) M. W. Davis and F. D. Richardson: *Trans. Faraday Soc.,* **55** (1959), 604.
30) A. Dusquenoy and F. Marion: *Compt. Rend.,* **a56** (1963), 2862.
31) A. Z. Hed and D. S. Tannhauser: *J. Electrochem. Soc.,* **114** (1967), 314, *J. Chem. Phys.,* **47** (1967), 2090.
32) N. G. Eror and J. B. Wagner: *J. Electrochem. Soc.,* **118** (1971), 1665.
33) N. Iwamoto, M. Takano and A. Adachi: unpublished paper.
34) A. Muan and S. Sōmiya: *Am. J. Sci.,* **2609** (1962), 230.
35) A. Muan and T. Katsura: *Trans. AIME,* **230** (1964), 74.
36) A. R. Stokes: *Proc. Phys. Soc.,* **61** (1948), 382.
37) J. Smuts: *JISI,* **204** (1966), 237.
38) W. Ruland: *Acta. Cryst.,* **14** (1961), 1180.
39) R. E. Watson and A. J. Freeman: ibid, **14** (1961), 27.
40) A. Muan and E. Osborn: "Phase Equilibria among Oxides in Steelmaking "Addison-Wesley, (1965).
41) C. Carel and P. Vallet: *Compt. Rend.,* **258** (1964), 3281.
42) C. Carel, D. Wiegel and P. Vallet: ibid, **260** (1965), 425.
43) J. Manenc, J. Bourgeot and J. Benard: ibid, **258** (1964), 4528.
44) F. Koch and J. B. Cohen: *Acta. Cryst.,* **B25** (1969), 275.
45) M. O'keeffe and M. Valigi: *J. Phys. Chem. Solids,* **31** (1970), 947.
46) J. P. Bocquet, M. Kawahara and P. Lacombe: *Compt. Rend.,* **265** (1967), 1318.
47) F. W. Jones: *Proc. Roy. Soc.,* **A16** (1938), 16.
48) R. E. Carter: *J. Am. Ceram. Soc.,* **42** (1959), 324.
49) H. Inoue, J. W. Tomlinson and J. Chipman: *Trans. Faraday Soc.,* **49** (1959), 796.